



## Characteristics of deep GPS signal fading due to ionospheric scintillation for aviation receiver design

Jiwon Seo,<sup>1</sup> Todd Walter,<sup>1</sup> Tsung-Yu Chiou,<sup>1</sup> and Per Enge<sup>1</sup>

Received 31 October 2008; revised 5 March 2009; accepted 19 March 2009; published 18 July 2009.

[1] Deep and frequent fading of Global Positioning System (GPS) signals caused by ionospheric scintillation is a major concern for aircraft navigation using GPS in the equatorial region during solar maximum. Aviation receivers use both code and carrier measurements to calculate position solutions. Deep signal fading can break a receiver's carrier tracking lock to a satellite channel. The lost channel cannot be used for position calculation until the receiver reacquires the channel and reestablishes tracking. A solar maximum data set analyzed in this paper demonstrates frequent deep signal fading of almost all satellites in view. This could significantly reduce the number of simultaneous tracked satellites and consequently decrease navigation availability. Forty-five minutes of strong scintillation, which was the worst scintillation period of a 9 day campaign at Ascension Island in 2001, are analyzed in this paper. The importance of short reacquisition time of the receiver is described. In order to design an aviation receiver with short reacquisition time under frequent deep signal fading, the characteristics of signal fading should be well understood. Fading duration and the time between deep fades are two important characteristics for GPS navigation. This paper presents a fading duration model based on real scintillation data. The time between deep fades observed in this data shows very frequent deep fades which can significantly reduce benefit of carrier smoothing filters of aviation receivers.

**Citation:** Seo, J., T. Walter, T.-Y. Chiou, and P. Enge (2009), Characteristics of deep GPS signal fading due to ionospheric scintillation for aviation receiver design, *Radio Sci.*, 44, RS0A16, doi:10.1029/2008RS004077.

### 1. Introduction

[2] The ionosphere has a practical importance to GPS applications because it influences transionospheric radio wave propagation. Among various phenomena of ionosphere, ionospheric scintillation [Crane, 1977] due to electron density irregularities can cause deep GPS signal fading. The carrier to noise density ratio ( $C/N_0$ ) of a satellite channel varies slowly without scintillation as in Figure 1 (top). However, if strong scintillation occurs,  $C/N_0$  fluctuates rapidly and sometimes drops more than 25 dB as in Figure 1 (bottom). Ionospheric amplitude and phase scintillation is not usually observed in the midlatitude region, but it is frequently observed in the equatorial region during solar maximum after local sunset [Basu and Basu, 1981; Aarons, 1982] and is potentially limiting to GPS navigation in the region.

[3] The data set used for this research contains frequent deep signal fading due to strong scintillation. The signal fades are deep enough to break a receiver's carrier tracking lock. Since the navigation system using GPS and Wide Area Augmentation System (WAAS) [Enge *et al.*, 1996] utilizes both code and carrier information, loss of carrier lock reduces navigation availability and continuity, especially when multiple satellite channels are lost simultaneously.

[4] Previous research showed that chance of multiple satellite loss is strongly dependent on a receiver's reacquisition time (J. Seo *et al.*, Ionospheric scintillation effects on GPS receivers during solar minimum and maximum, paper presented at International Beacon Satellite Symposium, International Union of Radio Science, Boston, Massachusetts, 11–15 June, 2007). This paper emphasizes the dependency using a severe scintillation data set. Given the dependency, it is important to design an aviation receiver to have a short reacquisition time in order to reduce the chance of simultaneous loss of multiple satellites.

<sup>1</sup>Department of Aeronautics and Astronautics, Stanford University, Stanford, California, USA.

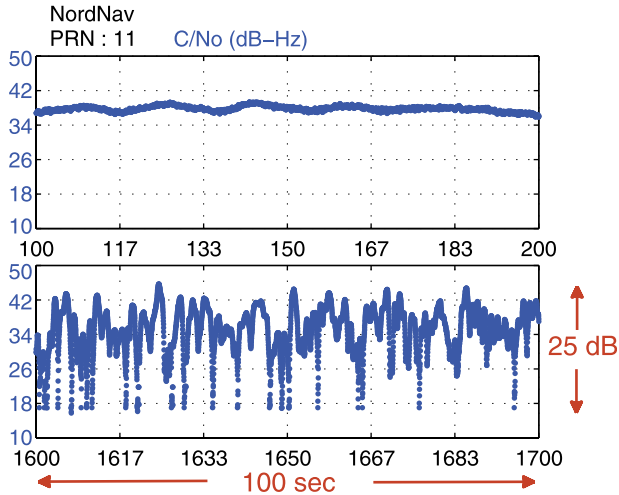


**Figure 1.** Example of deep signal fading due to ionospheric scintillation. Data collected on 18 March 2001 at Ascension Island.

[5] This paper presents a fading duration model that was developed based on scintillation data from the previous solar maximum. The fading duration model is useful as a guideline for developing a receiver with short reacquisition capability after a signal outage. There are several possible strategies for either maintaining lock during signal fading or quickly reacquiring after loss of lock. Doppler aiding [Chiou *et al.*, 2008] and Vector Phase Lock Loops (VPLL) (P. Henkel *et al.*, Multicarrier vector phase locked loop for robust carrier tracking, paper presented at 12th European Navigation Conference, European Group of Institutes of Navigation, Toulouse, France, 23–25 April, 2008) are being investigated to determine their effectiveness.

[6] Another important parameter related to navigation availability is the time between deep fades. Aviation receivers use carrier smoothing, also known as Hatch filtering (R. Hatch, The synergism of GPS code and carrier measurements, paper presented at 3rd International Geodetic Symposium on Satellite Doppler Positioning, New Mexico State University, Las Cruces, 8–12 February, 1982), to reduce noise levels on the code measurements. Frequent deep fades cause frequent resets of carrier smoothing filter, which shortens the effective smoothing times. Less smoothing leads to higher noise levels, and lower availability of the navigation operation. Examples of times between deep fades are analyzed in this paper and their potential impact on navigation is discussed.

## 2. Severe Scintillation Data Set

[7] The scintillation data were collected during the previous solar maximum period at Ascension Island in

the South Atlantic Ocean. The campaign was performed from 13 March 2001 to 26 March 2001 and reliable data was obtained for 9 days. T. Beach of the U.S. Air Force Research Laboratory (AFRL) provided  $S_4$  plots and raw Intermediate Frequency (IF) data for this research [Ganguly *et al.*, 2004]. The most severe scintillation period was selected based on the  $S_4$  index. The selected period was from 8:45 P.M. to 9:30 P.M. on 18 March 2001 (UTC, also local time). The analysis in this paper is based on this 45 min worst case data set.

[8] Raw IF data was collected using a NAVSYS DSR-100 receiver [May *et al.*, 1999] with a Rubidium frequency standard. The raw data was processed using a NordNav commercial software receiver [Normark and Stahlberg, 2005]. The 50 Hz  $C/N_0$  outputs from the NordNav receiver are used for this research. A benefit of raw IF data and postprocessing using a software receiver is that tracking loop algorithms and settings can be adjusted to maximize tracking capability for a specific data set. Raw IF data is ideal to investigate characteristics of weak signal for short timescales. The NordNav processing was set up to maximize its ability to track each signal into and out of each fade. Commercial and aviation receivers with more limited resources and running in real time, may not be able to track as deep into each signal fade or reacquire the signal after a fade as quickly. Despite the benefit, raw IF data size is very large and data storage is a problem for a long-term data collection campaign.

[9] As shown in Figure 2, seven (with red arrows) out of eight satellites were affected by severe scintillation in

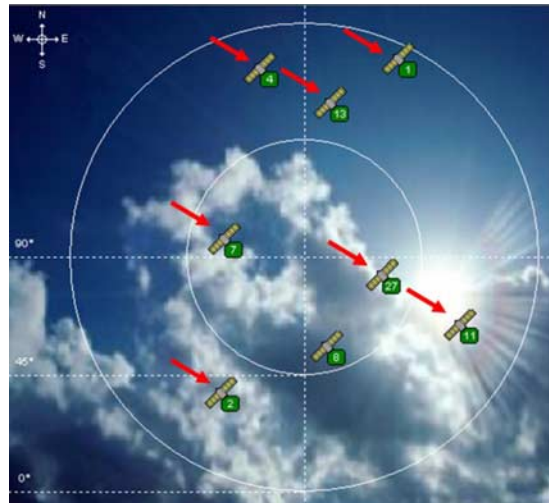


**Figure 2.** Satellites affected by scintillation. Seven out of eight satellite channels were affected during the 45 min of strong scintillation, which was the worst case from the 9 day campaign at Ascension Island.

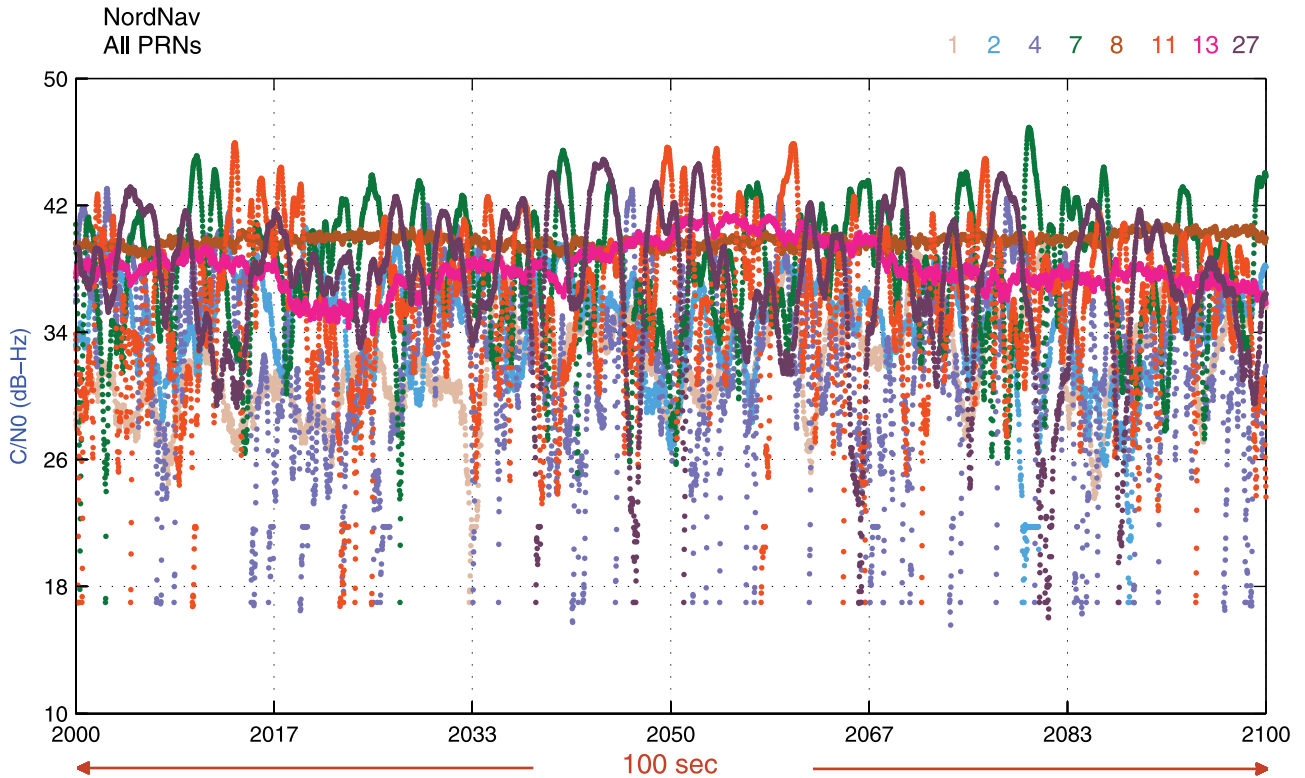


**Figure 3.**  $C/N_0$  outputs of all eight satellite channels during the strong scintillation (100 s example from the 45 min worst case data). 100 s is the carrier smoothing time constant of aviation receivers. The receiver experienced very frequent deep signal fades within 100 s.

this data set, which is a very stressing case. Figure 3 shows an example of  $C/N_0$  outputs of all eight satellite channels from a 100 s period of the severe scintillation data. Frequent deep signal fades of almost all channels are observed in Figure 3. As will be discussed in section 5, this data set has lower than typical  $C/N_0$  values.

### 3. Reacquisition Time and Number of Tracked Satellites

[10] The data shows that when strong scintillation occurs, almost all satellites in view could suffer from deep signal fading. However, it does not necessarily mean that a receiver fails to track multiple satellites simultaneously. As Figure 3 illustrates, deep signal fading of different satellites do not usually happen at the exact same time. Hence, if a receiver can reacquire a lost satellite before it loses other satellites, it can avoid simultaneous losses and consequently reduce the impact of scintillation on GPS navigation.

[11] Figure 4 shows the dependency of number of tracked satellites on a receiver’s reacquisition time for this data set. Reacquisition times from 1 s up to 20 s are

considered in Figure 4. The longer reacquisition times are simulated by discarding data after the  $C/N_0$  recovers from a deep fade. Whenever a deep fade occurs for a certain satellite channel during the 45 min period, a

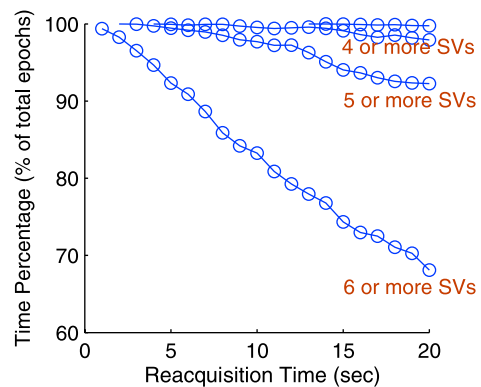


**Figure 4.** Number of tracked satellites according to various reacquisition times during the 45 min of severe scintillation. Shorter reacquisition time results in more satellites tracked.

receiver is assumed to lose the channel during predefined reacquisition time for the simulation of Figure 4. For example, 20 s reacquisition time means a 20 s loss of a satellite tracking after the deep signal fading ends. A precise definition of deep signal fading of this paper will be specified in section 4.

[12] The current WAAS MOPS [Radio Technical Commission for Aeronautics (RTCA), 2006] allows up to a 20 s reacquisition time for aviation receivers. However, if a 20 s reacquisition time is always assumed under the severe scintillation studied here, 4 or more satellites are tracked only 97.9% of the time. Five or more tracked satellites occurs only 92.3% of the time and 6 or more satellites only 68.1%. Note that a receiver has to track at least 4 satellites with good geometry to navigate using GPS. The low percentages of sufficient number of satellites tracked may not provide enough availability to enable operations during times of expected strong scintillation. If a receiver can always reacquire the lost channel within 2 s for example, the result is much better. In this case, a receiver always tracks 5 or more satellites during the same strong scintillation period and tracks 6 or more satellites 98.3% of the time. This result clearly demonstrates the benefit of shorter reacquisition time.

[13] In order to develop strategies to design a receiver with a short reacquisition time following a brief outage, it is helpful to understand characteristics of signal fading in the strong scintillation environment. Among various characteristics of deep signal fading due to scintillation, fading duration and time between deep fades directly affect GPS navigation and aviation receiver design, which will be discussed in sections 5 and 6.

#### 4. Definition of Deep Signal Fading

[14] Before investigating the characteristics of deep GPS signal fading, it is necessary to make a proper definition of deep fading. If a signal fade is deep enough to break the receiver's carrier tracking loop, the fade can be detrimental to GPS navigation. Hence, at least in GPS navigation's point of view, it is logical to define deep fading in the context of a receiver's carrier tracking loop performance.

[15] The NordNav software receiver used on this data set almost always lost carrier lock when the minimum  $C/N_0$  of a fading is below 20 dB-Hz, so a deep fade in this paper is defined as fading that results in a minimum  $C/N_0$  of 20 dB-Hz or less. Among various  $C/N_0$  fluctuations, only deep fades are selected and samples below the threshold are marked in red in Figure 5. A fading selection algorithm using local minimum and maximum comparison was developed to specify begin and end points of a single fading.

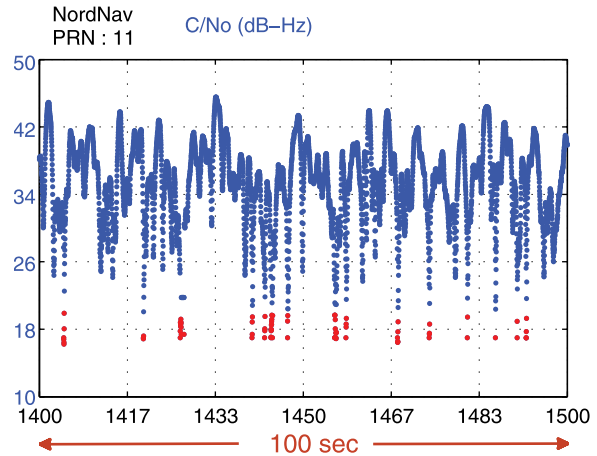


**Figure 5.** Example of deep signal fades according to the definition of this paper. Samples below 20 dB-Hz are marked in red.

[16] Since different receivers have different tracking loop performances, other definitions of deep fading may make more sense for other types of receivers. Effects of different definitions of deep fading on the results of this paper will be also discussed in section 7 after analyzing two important characteristics of deep fading in sections 5 and 6.

#### 5. Fading Duration Model

[17] This section discusses properties of fading duration which is one of two important characteristics of deep signal fading that directly affect GPS navigation and aviation receiver design. A receiver could reduce the reacquisition time by it retaining its tracking information during short fading periods. *Chiou et al.* [2008] demonstrated good performance from a Doppler-aided frequency lock loop as a means of coasting during deep signal fading caused by scintillation. Coasting is defined here to be a period of time over which the receiver can keep its tracking loops close enough to the correct value that the receiver can immediately reacquire the signal when the power level is restored above the tracking threshold of the receiver. Although coasting is a good strategy for rapid reacquisition after a loss of lock, the goal of using coasting to avoid declaring a cycle slip altogether carries more risk. Particularly for aviation applications, more study is needed to ensure that such a strategy does not mask unexpected satellite or user behavior.

[18] The idea of coasting is particularly useful if the signal outage is brief. The accuracy of the expected tracking information degrades as the coasting time increases. A guideline about the duration of signal outages is helpful for aviation receiver manufacturers to

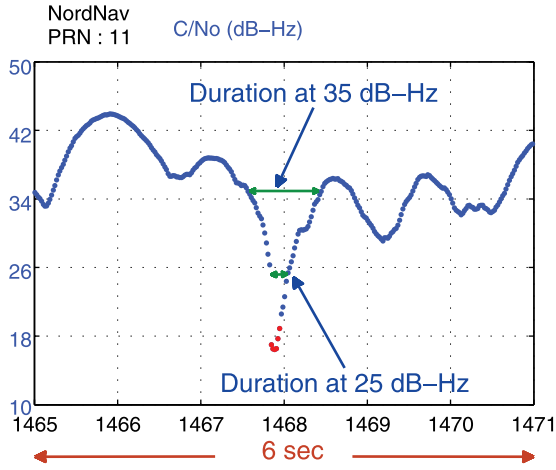


**Figure 6.** Definition of fading duration. Fading duration is obtained for every deep fade identified. The fading durations at lower absolute  $C/N_0$  values are shorter.

develop proper coasting algorithms. If the fading duration is long, a receiver may still be able to coast with the help of high-grade Inertial Measurement Unit (IMU). However, this solution may be prohibitively expensive for most users.

[19] The fading duration in this paper is defined as time to recover the previous  $C/N_0$  value when deep signal fading occurs. According to this definition, fading duration is not a single number for a single fade but is obtained at each 50 Hz  $C/N_0$  data point. Figure 6 shows

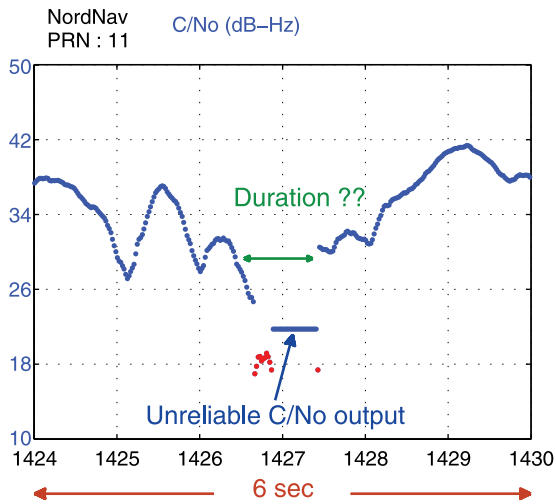


**Figure 7.** Examples of unreliable  $C/N_0$  outputs from NordNav receiver. These unreliable durations are not included in the statistics of this paper.

fading durations at 25 dB-Hz and 35 dB-Hz as examples. The fading duration at 35 dB-Hz is about 1 s and the fading duration at 25 dB-Hz is about 0.2 s in this example. Note that these  $C/N_0$  values are absolute  $C/N_0$  values and not a relative depth of fade. This approach was chosen because a receiver’s tracking loop performance depends on the absolute  $C/N_0$  level.

[20] Ideally, the fading duration could be obtained at every 50 Hz data point of every deep fade. Unfortunately, the actual response of the NordNav software receiver is not always ideal. For example, the NordNav receiver sometimes outputs unreliable  $C/N_0$  values as seen in Figure 7. Consecutive constant  $C/N_0$  outputs indicate the NordNav receiver does not process  $C/N_0$  correctly. The fading duration is not well defined in this case. Since these unreliable data points do not describe the physics of ionosphere, they have to be separated from reliable  $C/N_0$  outputs to obtain meaningful statistics of fading duration for this data set.

[21] Fading durations at all  $C/N_0$  outputs for all satellites during the 45 min data set are plotted in Figure 8. The blue data points in Figure 8 represent fading durations at reliable  $C/N_0$  outputs and the red points represent fading durations at unreliable  $C/N_0$  outputs. The number of reliable data points is 18,502 which is 78% of the total number of data points.

[22] Now the statistics of fading duration at each  $C/N_0$  value for this data set can be obtained. The top histogram of Figure 9 is generated using only reliable data points within 1 dB around a  $C/N_0$  of 25 dB-Hz from data in Figure 8. Figure 9 (top) shows that the median of fading duration at 25 dB-Hz was 0.29 s and the 95th percentile was 0.88 s. When 1 dB around 30 dB-Hz is considered, the bottom histogram of Figure 9 is generated. In this case, the

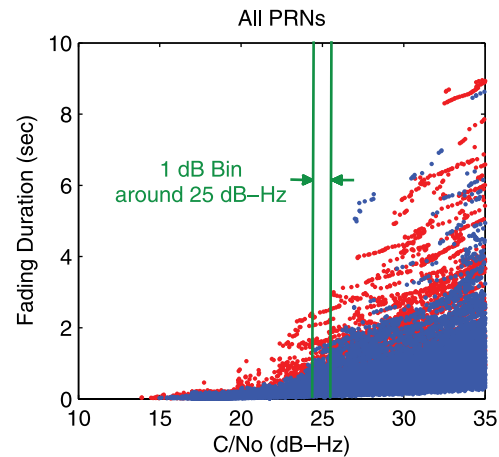


**Figure 8.** Fading durations obtained at all  $C/N_0$  data points of deep fades. Only reliable data points (blue points) are considered for statistics.

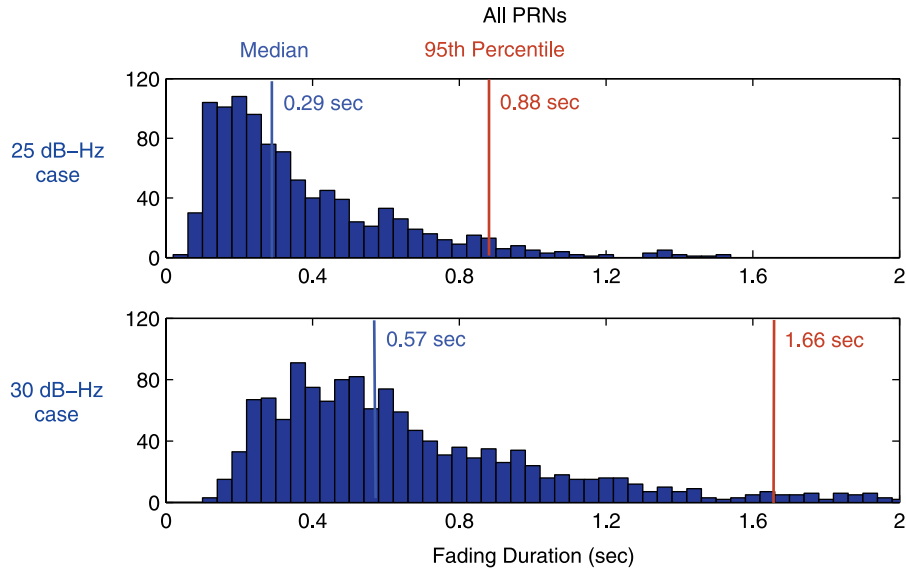


**Figure 9.** Histograms of fading durations at 25 dB-Hz and 30 dB-Hz. Medians and 95th percentiles of fading durations are obtained from the histograms.

median and 95th percentile of fading duration were longer than the 25 dB-Hz case as expected from Figure 6.

[23] Median and 95th percentile values were calculated at other  $C/N_0$  values from 15 dB-Hz to 30 dB-Hz to

develop an empirical fading duration model shown in Figure 10. Statistics of fading durations were obtained at each integer value of  $C/N_0$  and linearly interpolated. Note that this model has information of fading duration

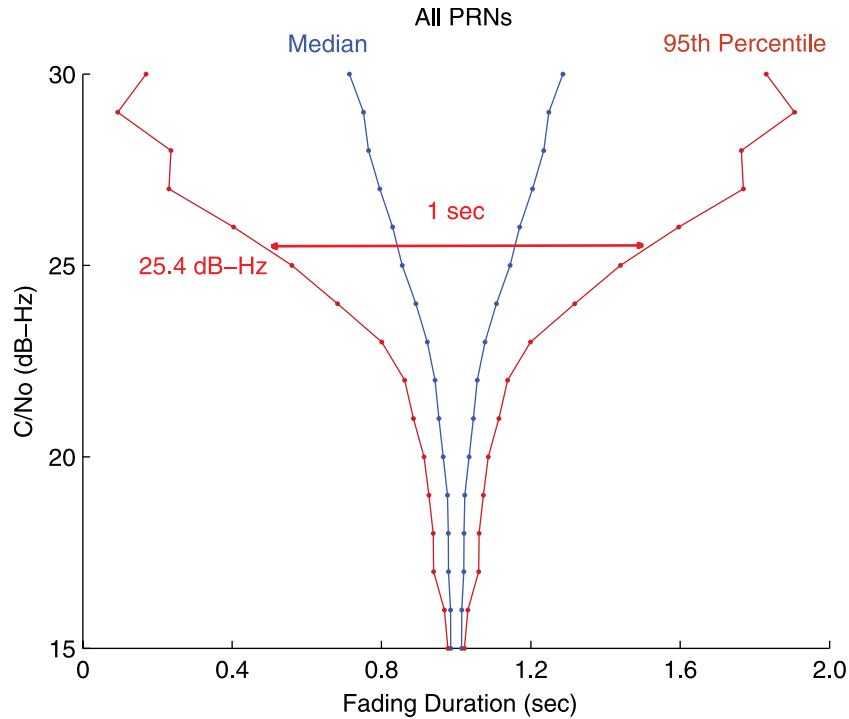


**Figure 10.** Empirical fading duration model. This model shows median and 95th percentile of fading durations at each  $C/N_0$  value.

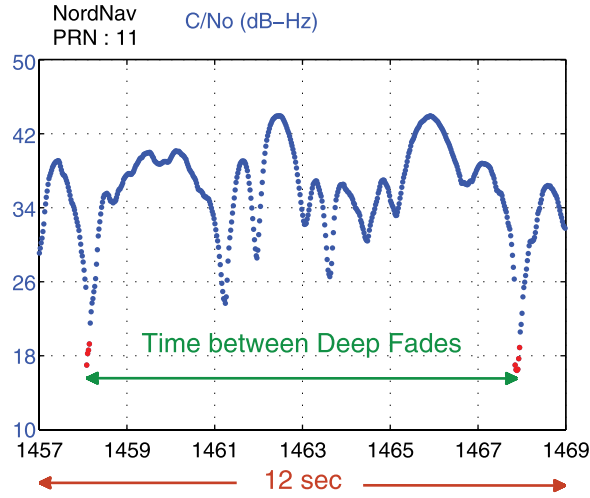


**Figure 11.** Definition of time between deep fades.

only at each  $C/N_0$  value but the model does not have information about the actual shape of fading. In Figure 10 it is shown as being symmetrical although this will not be true in general.

[24] There are several ways to interpret this model. If a receiver loses carrier lock at 25.4 dB-Hz for example, the receiver can expect the signal to return to the same level of  $C/N_0$  after 1 s in 95% of the deep fades. Another point of view is that if a receiver can coast for 1 s, if that receiver was also able to track down to at least 25.4 dB-Hz, it would have successfully handled 95% of the deep fades in this data set. There is a relationship between a receiver's sensitivity and required coasting time. If a receiver is more sensitive, in other words if a receiver can track signal at lower  $C/N_0$ , the required coasting time would be smaller for the same level of functionality.

[25] The fading duration model shows signal environment under strong scintillation but receivers' response to the same signal environment can be very different from each other. Depending on receiver design and hysteresis, a receiver requires different time for reacquisition after recovering the same  $C/N_0$  level. Reacquisition capability of a receiver characterized by its reacquisition time has important relationship with number of tracked satellites under scintillation as discussed in section 3.

[26] This fading duration model is generated from limited number of data points from the previous solar maximum. It is observed that the 95th percentile of fading duration at 28 dB-Hz is slightly smaller than 27 dB-Hz case, which is not intuitive. This result is due to limited number of samples. In addition, this sampling derives from a single period of scintillation at a single location. It is believed to be loosely representative of severe scintillation and that much more often a user would encounter less severe effects. Nevertheless,

the authors acknowledge that longer and deeper fades are possible. Platform motion, in particular, can potentially lead to much longer fades under the scenario that platform motion is exactly lined up with motions of the satellite and the electron density irregularity.

[27] Another important point to consider is the uncertainty of the  $C/N_0$  levels. The raw IF data for this research was collected by an early IF capture technology incorporating one-bit sampling, narrow bandwidth, and aliasing caused by a low sampling frequency. After comparing  $C/N_0$  values of the scintillation data collected with DSR-100 in 2001 and nominal data collected with NordNav IF recorder in 2008, about an 8 dB difference was observed. This observation implies that about an 8 dB improvement may be attainable with current receiver technology such as multibit sampling, a wide bandwidth, a better front end, and a better frequency plan. If this current receiver technology is taken into account, the vertical axis of the fading duration model could be adjusted from 15 dB-Hz  $\sim$  30 dB-Hz to 23 dB-Hz  $\sim$  38 dB-Hz. The fading duration model of Figure 10 is still meaningful as a conservative model when one does not consider any benefit from technology improvement since 2001.

## 6. Time Between Deep Fades

[28] Another important characteristic of fading is the time between deep fades because it is related to the effective carrier smoothing time of the aviation receiver. An aviation receiver using GPS and WAAS smoothes its code measurements with less noisy carrier measurements using a Hatch filter (Hatch, presented paper, 1982) with a 100 s time constant. In theory, the measurement noise can be reduced as much as factor of 10 with this carrier smoothing technique. In practice, the reduction is found to be closer to half that value [Murphy *et al.*, 2005]. With a 100 s time constant, the Hatch filter needs to continuously operate for couple of hundred seconds without cycle slip to converge to its floor level. If a receiver loses carrier lock frequently within the 100 s smoothing period, the Hatch filter is frequently reset and cannot reduce code noise to desired level.

[29] The definition of time between deep fades of this paper is the time between minimum  $C/N_0$  values of two consecutive deep fades as shown in Figure 11. The histogram in Figure 12 is obtained using time between deep fades of all satellite channels during the strong scintillation. This histogram shows that time between deep fades is very short and the median is only 5.3 s which is far shorter than the 100 s smoothing time constant of aviation receivers. Five seconds of smoothing reduces measurement noise less than 10%.

[30] A receiver with the desired reacquisition capability may track enough satellites even during strong

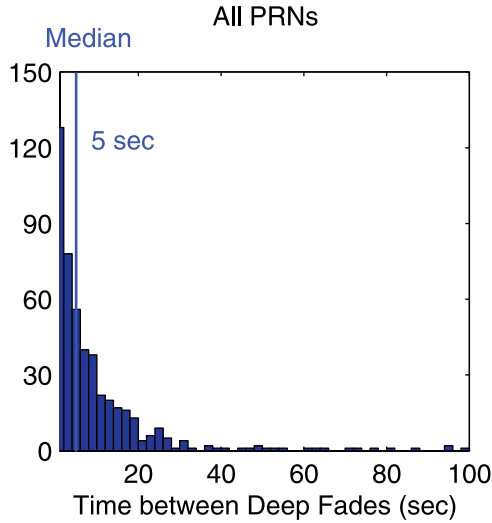


**Figure 12.** Histogram of time between deep fades during strong scintillation. The median of time between deep fades during the 45 min of strong scintillation is only 5 s.

scintillation. However, the high measurement noise due to frequent resetting of the Hatch filter is also a problem. The Hatch filter has to be reset whenever a cycle slip occurs. In order to guarantee aviation integrity, ambiguous carrier information while in a deep fade cannot be used upon reacquisition for carrier smoothing purposes. The very frequent deep fades observed in this research indicate that the availability of precision approach of aircraft may be significantly impacted during strong scintillation in the equatorial region.

### 7. Effects of Different Definitions of Deep Fading

[31] Deep fading in this paper so far has meant a signal fading in which the minimum  $C/N_0$  is less than 20 dB-Hz. This definition is well suited to the NordNav software receiver because it loses carrier lock in this situation. However, other receivers could lose carrier lock at higher  $C/N_0$ . Signal fades that are less deep could also be harmful to those receivers.

[32] Figure 13 presents deep fades in red according to three different definitions. Figure 13 (top) is the same as

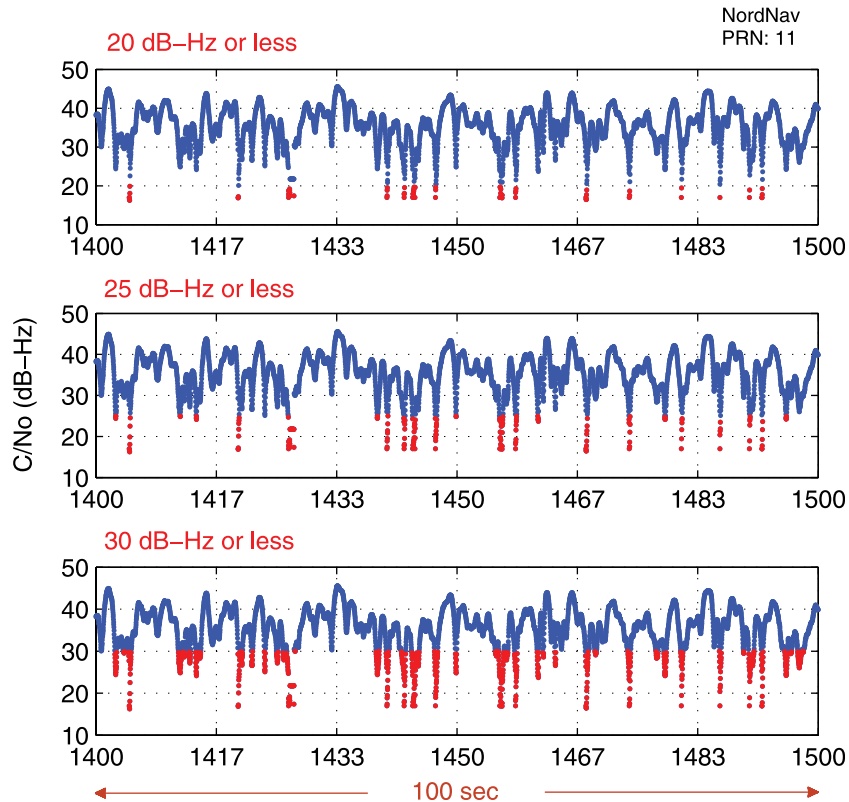


**Figure 13.** Comparison of different definitions of deep fading. When applying higher thresholds, more signal fluctuations are considered to be deep fading.

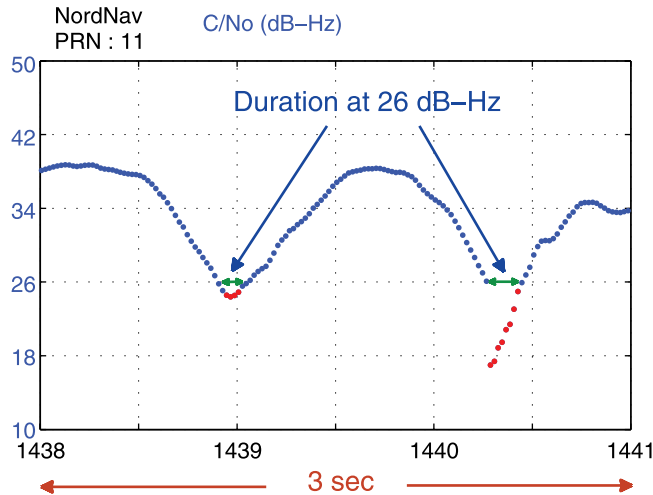


**Figure 14.** Effect of shallower fading on observed statistics. The shorter duration of the shallower fading on the left at the same  $C/N_0$  level yields less conservative statistics of fading durations.

previously defined which has minimum  $C/N_0$  of 20 dB-Hz or below (Figure 5). Figure 13 (middle) shows deep fading in which the defined fading has minimum  $C/N_0$  of 25 dB-Hz or below. Figure 13 (middle) contains more deep fades shown in red. Figure 13 (bottom) contains even more deep fades because the deep fading in Figure 13 (bottom) is defined as a minimum  $C/N_0$  of 30 dB-Hz or below. Remember that  $C/N_0$  values here are all absolute values. This was chosen because a receiver's tracking loop performance is related to absolute  $C/N_0$ , not relative  $C/N_0$  drop. Hence, lower absolute  $C/N_0$  value here indicates deeper signal fading.

[33] If the minimum  $C/N_0$  of 25 dB-Hz or below is defined as deep fading as in Figure 13 (middle), the first fade of Figure 14 is now considered as a deep fade. It was not included in the statistics of the fading duration model (Figure 10) because Figure 10 only considered fades with minimum  $C/N_0$  of 20 dB-Hz or below. Including shallower fades into the analysis creates less conservative statistics of fading duration. Shallower fades usually have shorter fading durations for the same  $C/N_0$  as shown in Figure 14. Hence, mean and 95th percentile values at the same  $C/N_0$  would be smaller and consequently the fading duration model of Figure 10 would become sharper when shallower fades are taken into account. This provides a less conservative guideline for required coasting time.

[34] However, the time between deep fades becomes shorter when including shallower fades into our analysis. The median time between deep fades is 4.3 s when a minimum  $C/N_0$  of 25 dB-Hz or below is considered to be deep fading. This is slightly shorter than the 5.3 s of 20 dB-Hz or below case presented in section 6. If a

minimum of 30 dB-Hz or below is considered as in Figure 13 (bottom), the median of time between deep fades decreases to only 2.7 s.

[35] Consequently, the fading duration model of Figure 10 remains a conservative representation of the data. Fade durations of order 1 s are to be expected during periods of severe scintillation. The time between deep fades does not change significantly if a receiver can maintain carrier lock down to 25 dB-Hz, but if a receiver loses carrier lock above 25 dB-Hz, time between deep fades becomes even shorter. However, measurement noise levels after 5.3 s of smoothing or 2.7 s of smoothing would not be significantly different. Both smoothing times are already very short compared to the filter warm-up time.

## 8. Conclusions

[36] Tracking at least 4 satellites is a basic requirement for GPS navigation. A receiver that loses too many satellites due to the influence of scintillation cannot meet this goal. However, since deep fades are typically short in duration and do not necessarily overlap, a receiver that can reacquire lost channels within reasonably short time can track enough satellites to navigate even during strong scintillation. This does not guarantee that the quality of the navigation will be sufficient to support the desired operation. The level of measurement noise and geometry of the tracked satellites are also important considerations.

[37] This paper examined an empirical fading duration model based on real scintillation data from previous solar maximum to provide a guideline for coasting time. The model provides the required coasting time depending on

a receiver's sensitivity and can be used by aviation receiver manufacturers to develop suitable coasting strategies to reduce the impact of deep signal fading. The fading duration model of this paper is compatible with other research [El-Arini et al., 2003] which reports about 1 s fading duration at 10 dB fading in Naha, Japan on 20 March 2002, although their approach to define and calculate fading duration is different from this paper.

[38] The short duration between fades is worrisome for the precision approach of aircraft. Measurement noise level is also an important parameter for determining operational availability. The benefit of conventional carrier smoothing to reduce noise will be significantly impacted due to very frequent deep fades as observed during the severe scintillation period analyzed here. High availability of precision approach may be difficult to achieve during periods of expected strong scintillation in equatorial regions close to the solar maximum. This effect is still under investigation to better quantify the impact.

[39] **Acknowledgments.** The authors gratefully acknowledge the Federal Aviation Administration (FAA) CRDA 08-G-007 for supporting this research and Theodore Beach, AFRL, for providing the data set. The opinions discussed here are those of the authors and do not necessarily represent those of the FAA or other affiliated agencies.

## References

- Aarons, J. (1982), Global morphology of ionospheric scintillations, *Proc. IEEE*, 70, 360–378, doi:10.1109/PROC.1982.12314.
- Basu, S., and S. Basu (1981), Equatorial scintillations—A review, *J. Atmos. Terr. Phys.*, 43, 473–489, doi:10.1016/0021-9169(81)90110-0.
- Chiou, T.-Y., J. Seo, T. Walter, and P. Enge (2008), Performance of a Doppler-aided GPS navigation system for aviation applications under ionospheric scintillation, in *Proceedings of 21st International Technical Meeting, Savannah, GA, 16–19 September*, Inst. of Navig., Manassas, Va.
- Crane, R. K. (1977), Ionospheric scintillation, *Proc. IEEE*, 65, 180–199, doi:10.1109/PROC.1977.10456.
- El-Arini, M. B., R. S. Conker, S. D. Ericson, K. W. Bean, F. Niles, K. Matsunaga, and K. Hoshinoo (2003), Analysis of the effects of ionospheric scintillation on GPS L2 in Japan, in *Proceedings of 16th International Technical Meeting, Portland, OR, 9–12 September*, Inst. of Navig., Manassas, Va.
- Enge, P., T. Walter, S. Pullen, C. Kee, Y.-C. Chao, and Y.-J. Tsai (1996), Wide area augmentation of the global positioning system, *Proc. IEEE*, 84, 1063–1088, doi:10.1109/5.533954.
- Ganguly, S., A. Jovancevic, A. Brown, M. Kirchner, S. Zigic, T. Beach, and K. Groves (2004), Ionospheric scintillation monitoring and mitigation using a software GPS receiver, *Radio Sci.*, 39, RS1S21, doi:10.1029/2002RS002812.
- May, M., A. Brown, and B. Tanju (1999), Applications of digital storage receivers for enhanced signal processing, in *Proceedings of 12th International Technical Meeting, Nashville, TN, 14–17 September*, Inst. of Navig., Manassas, Va.
- Murphy, T., M. Harris, P. Geren, T. Pankaskie, B. Clark, and J. Burns (2005), More results from the investigation of airborne multipath errors, in *Proceedings of 18th International Technical Meeting, Long Beach, CA, 13–16 September*, Inst. of Navig., Manassas, Va.
- Normark, P.-L., and C. Stahlberg (2005), Hybrid GPS/Galileo real time software receiver, in *Proceedings of 18th International Technical Meeting, Long Beach, CA, 13–16 September*, Inst. of Navig., Manassas, Va.
- Radio Technical Commission for Aeronautics (RTCA) (2006), Minimum operational performance standards for global positioning system/wide area augmentation system airborne equipment, *Doc. DO-229D*, Washington, D. C.
- T.-Y. Chiou, P. Enge, J. Seo, and T. Walter, Department of Aeronautics and Astronautics, Stanford University, Stanford, CA 94305, USA. (jwseo@cs.stanford.edu)